Volume 52 http://acousticalsociety.org/

Acoustics 2023 Sydney

185th Meeting of the Acoustical Society of America

Sydney, Australia

4-8 December 2023

***Structural Acoustics and Vibration: Paper 4aSA2**

Experimental measurements of stress in an Acoustic Black Hole using a laser doppler vibrometer

Archie Keys
ISVR, University of Southampton School of Engineering, Southampton, Hampshire, SO17 1BJ, UNITED KINGDOM; a.keys@soton.ac.uk

Jordan Cheer
University of Southampton School of Engineering, Southampton, Hampshire, SO17 1BJ, UNITED KINGDOM; j.cheer@soton.ac.uk

Acoustic Black Holes (ABHs) make use of modifications to a structure to effectively decrease the structural wavespeed, thus increasing the effect of damping material applied in the ABH taper region, resulting in greater vibration attenuation. The most common way in which this is implemented is by gradually reducing the thickness of the structure over a finite interval, to a very thin tip. The focusing effect of the ABH results in high amplitude vibrations occurring in the thin part of the structure, resulting in high stresses and raising significant concerns about fatigue life. This paper presents an experimental assessment of stress in the taper section of an ABH used to terminate a uniform beam, using laser doppler vibrometer measurements to avoid the mass loading associated with accelerometers or strain gauges. A calculation of stress using Euler-Bernoulli beam theory is then presented, and the validity of this approach is assessed for a thick damping layer applied to a thin structure. A comparison is then made to predictions from a numerical model, in order to validate the results from the experimental measurements.

***POMA Student Paper Competition Winner**

Published by the Acoustical Society of America

 https://doi.org/10.1121/2.0001829

1. INTRODUCTION

In engineering applications it is often desirable to reduce the level of vibration in a structure, since high levels can result in issues such as structural fatigue or the radiation of unwanted noise. Traditional methods for the attenuation of such vibration usually either increase the mass of the structure, or use passive damping treatments to dissipate the energy as heat. In many applications it is undesirable to increase the mass of a structure, and passive damping treatment is only effective when the wavelength of vibration is comparable to the size of the treatment. Acoustic Black Holes (ABHs) are structural features that are able to effectively attenuate vibration over a broad range of frequencies, while reducing the mass of a structure. This characteristic behaviour is achieved through modifications to the structure which act to decrease the speed of an incident wave, decreasing its wavelength and thus increasing the effectiveness of any damping treatment applied.

The concept of an ABH was first introduced by Mironov,[1] who analytically demonstrated that a gradually tapering thickness applied to the free edge of a plate will result in a zero reflection condition if the thickness of the taper at the termination is zero. This occurs since the speed of a wave travelling through a plate or beam is proportional to the square root of the thickness. In practice a zero thickness termination is not realisable, and Mironov showed that with a finite thickness termination to a tapering profile the majority of the wave energy is still reflected. However, it was later demonstrated that a practical ABH taper with finite tip height can result in effective vibration attenuation if a thin, viscoelastic damping layer is applied in the ABH taper region.[2] The tapering thickness of the ABH results in a reduction in the wavelength of an incident wave, thus increasing the dissipation of energy by the applied damping treatment.

The effectiveness of ABHs as vibration attenuators has been demonstrated thoroughly in the literature,[2–4] however there are concerns about the strength of the structure given that the performance of an ABH is strongly related to the thinness of its tip. The strength of an ABH under static load has been investigated, and configurations that reduce static stress have been proposed.[5–7] More recently, the fatigue behaviour of an ABH under dynamic loading has been investigated,[8] and a design for a modified ABH profile that reduces fatigue has been proposed.[9] Fatigue has been identified as a concern for ABHs due to the energy focusing effect that results in large amplitude waves occurring in the thin part of the ABH taper, which cause high levels of stress. It is therefore important that analysis is carried out to assess the dynamic stresses that occur in the ABH taper, so that fatigue failure of the structure can be prevented when implemented in environments that experience high amplitude vibration.

This paper outlines a method for the measurement of dynamic stress in an ABH used to terminate a uniform beam when subjected to a white noise load. A method for the calculation of dynamic stress in a structure using deflection data is outlined, before being implemented to assess the stress in a numerical model of an ABH. Experimental measurements of velocity across a grid of points on an ABH taper are taken, and used to experimentally validate the numerical results. Conclusions are drawn based on analysis of both the numerical and experimental results.

2. STRESS CALCULATION METHOD

The method used to estimate stress based on velocity data at discrete points on the taper is outlined in this section, detailing how Euler-Bernoulli beam theory can be used to calculate bending stress from the second spatial derivative of beam deflection.

Traditional methods for the measurement of stress in a structure use strain gauges, however this has two drawbacks when applied to an ABH taper. Firstly, the ABH taper is very thin towards the tip, so the mass of the strain gauge may become significant when taking measurements. Another limitation is that strain gauges measure over a distributed area, which may limit the physical insight into stresses that are highly localised. Both of these problems can potentially be overcome by using a laser doppler vibrometer to measure the

Figure 1: Numerical model viewed with the z-axis out of the page, showing the grid of points in the ABH taper section used in the stress calculation on the right hand side.

velocity experimentally over a grid of points and estimating the stress from this distributed measurement.

Euler-Bernoulli beam theory gives a simple analytical relationship between the bending stress in a beam, σ, and the second spatial derivative of beam deflection, w, as[11]

$$\sigma = -zE_a \frac{d^2w}{dx^2} \tag{1}$$

where z is the distance between the neutral axis of the structure and the point at which stress is being evaluated and E_a is the Young's modulus of the material from which the beam is constructed. In the case of the ABH taper implemented here, the distance from the neutral axis of the structure to the point of stress measurement is equal to half of the thickness profile, $h(x)$, when stress is evaluated on the surface of the taper.

In order to obtain the second spatial derivative of beam deflection, velocity data from a 13 by 9 grid of points across the ABH taper, which gives a 0.5 cm spacing in both directions, is used as shown in Figure 1. The complex velocity data from these points can be converted into complex deflection in the frequency domain by dividing by jω. The second spatial derivative of deflection can then be calculated using a simple gradient function, and the stress across the surface of the ABH taper can then be calculated according to Equation 1.

3. NUMERICAL MODEL

This section describes the numerical model that has been used to obtain predictions of the stress in an ABH taper, including the parameters that define the geometry and physical characteristics of the structure. The method outlined in Section 2 is then applied to numerical data, and the calculated stress is compared to the stress directly evaluated by the numerical model in order to assess the suitability of the method.

For the work described in this paper, a 2D finite element model of a uniform aluminium beam with an ABH termination has been implemented using COMSOL multiphysics software. The dimensions of the structure are defined in Figure 2 and the values are listed in Table 1. The thickness of the structure is constant in the uniform beam section, while the ABH taper thickness decreases according to a power law from the uniform beam thickness, $h(0)$, to the tip height, h_{tip}, according to

$$h(x) = \left(\frac{l_{ABH} - x}{l_{ABH}}\right)^{\mu} (h_0 - h_{tip}) + h_{tip}. \tag{2}$$

It has been demonstrated that the amount of damping material applied to an ABH taper, as well as the regions over which it is applied, have a significant impact on ABH performance.[10] It is therefore important that the numerical model used for this work accurately replicates the damping treatment used in the experimental validation, where a constant thickness layer of viscoelastic material is applied over the ABH taper.

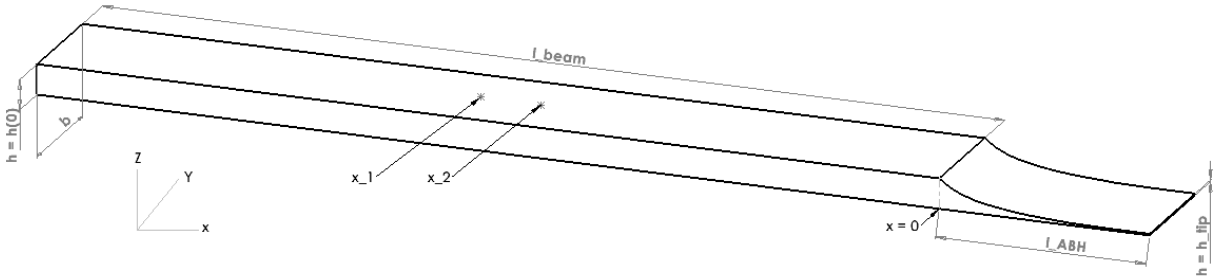

Figure 2: Beam with ABH termination: definition of geometric parameters.

Table 1: Parameter values as defined in Fig. 1

Parameter	Symbol	Value
Beam height	$h(0)$	10 mm
Beam length	l_{beam}	300 mm
Beam width	b	40 mm
ABH length	l_{ABH}	70 mm
ABH tip height	h_{tip}	0.6 mm
ABH power law	μ	4
Excitation force	F	1 N

The numerical model used here represents the damping via an isotropic loss factor in the ABH taper, and, therefore, to represent the constant thickness damping treatment this is scaled along the length of the taper according to its thickness. The isotropic loss factor at each point on the ABH taper, $\eta(x)$, is defined as

$$\eta(x) = \frac{\eta_0 \times h_{tip}}{h(x)}, \tag{3}$$

where η_0 is a scalar value defining the loss factor at the ABH tip.

Another material property that needs to be accurately modelled to ensure the numerical model matches the experimental set-up is the stiffness due to the applied viscoelastic damping material. The thickness of the applied damping layer is approximately 3 mm, which is considerably thicker than the ABH tip, therefore the additional stiffness added to the taper by the damping material will have a significant impact on the behaviour of the structure. The numerical model approximates this effect by implementing an equivalent stiffness model, where the Young's modulus in the ABH taper is adjusted so that the stiffness of the structure is the same as that of the experimental beam with the damping layer applied. The Young's modulus at position x in the ABH taper, E_{eq}, is given by

$$E_{eq}(x) = E_a + \frac{E_d I_d}{I_a(x)}, \tag{4}$$

where E_a is the Young's modulus of aluminium, E_d is the Young's modulus of the damping material, I_d is the second moment of area of the damping layer and $I_a(x)$ is the second moment of area of the ABH taper. In order to account for the mass added to the experimental structure by the damping layer, a uniform mass distribution of 11.9 g is added to the ABH taper section in the numerical model.

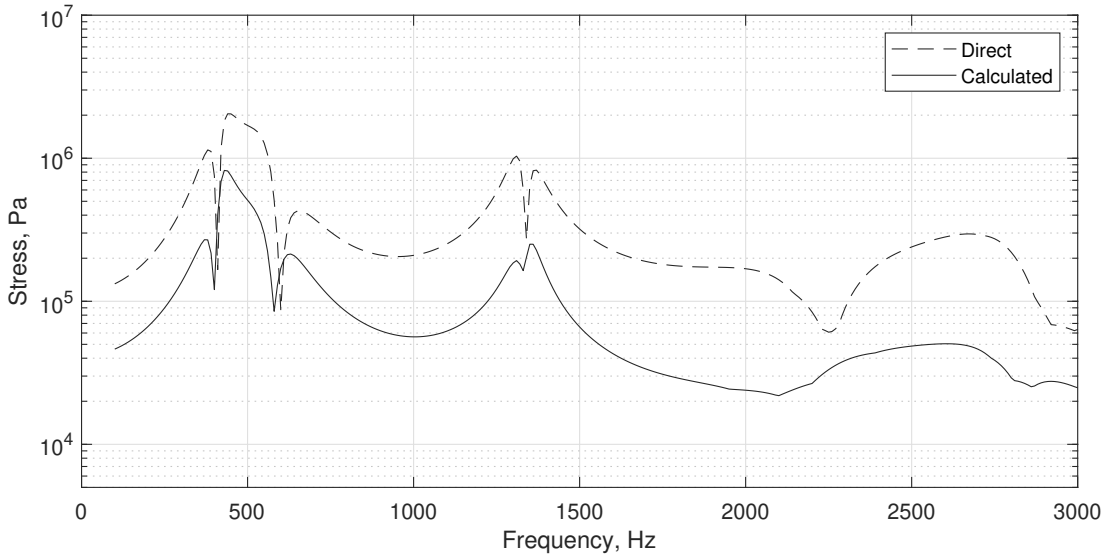

Figure 3: Directly exported stress (dashed line) and calculated stress (solid line) at a point in the ABH taper against frequency.

A. SIMULATION RESULTS

The numerical model described in this section has been used to estimate the stress in the ABH taper, as well as assessing the accuracy of the stress calculation method. A force has been applied to the non-ABH end of the structure, evenly distributed across a small ring to replicate the way in which the force is applied experimentally. The stress calculation is carried out over a frequency range of 100 Hz to 10 kHz, however the results of the calculation are only shown up to 3 kHz since the level of stress above this frequency drops off significantly.

Figure 3 shows the stress obtained using the numerical model, comparing the stress directly evaluated in the model and that calculated using the method described in Section 2. Examination of the results shows good agreement between the calculated and direct stress values in terms of the shape of the plots, however, the calculated stress value consistently underestimates the direct stress from the model. There is also a small shift in the frequencies at which peaks and troughs in the stress appear. It is thought that the differences between the direct and calculated stress are due to the assumption that an ABH behaves as an Euler-Bernoulli beam. The assumption most clearly violated by an ABH structure, due to the tapering thickness, is that an Euler-Bernoulli beam must have constant cross-section.[11] It is possible that this assumption could account for the significant difference between the calculated and direct stress from the numerical model, but requires further investigation.

4. EXPERIMENTAL MEASUREMENTS

This section describes the experimental set-up used to obtain measurements of velocity over a grid of points on an ABH taper. These measurements are used to calculate the stress in the ABH taper using the method outlined in Section 2, and comparisons are made to the estimate calculated using the responses from the numerical model.

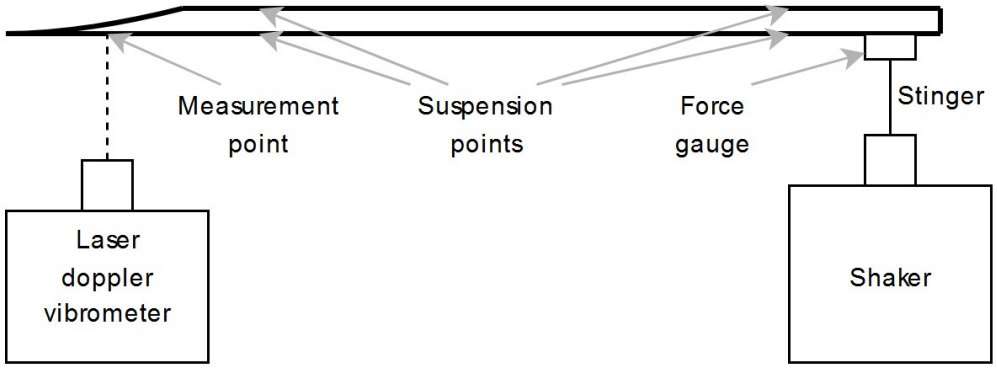

Figure 4: Diagram showing the elements of the experimental set-up used to obtain measurements of ABH taper velocity.

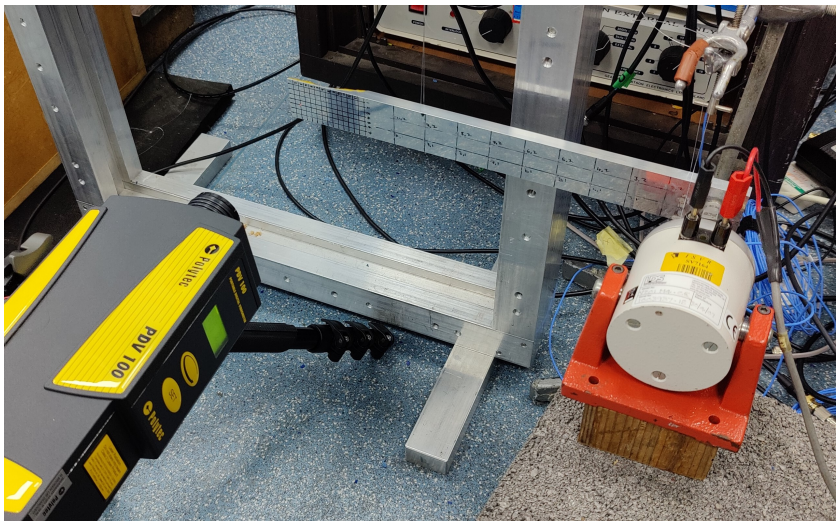

Figure 5: Image showing the experimental set-up used to obtain measurements of ABH taper velocity.

A. EXPERIMENTAL SET-UP

The experimental set-up used to obtain measurements of the ABH taper velocity is shown in Figures 4 and 5. It consists of a uniform aluminium beam terminated by an ABH taper with a thickness profile defined by Equation 2. The beam is manufactured from aluminium alloy 8082-T6, with the ABH taper being CNC milled to ensure accuracy, and 11.9 g of Henley's plastic compound applied to the ABH taper region to act as a damping layer. The beam is suspended using two loops of fishing wire in the positions marked on Figure 4, to approximate free boundary conditions. A shaker is connected to the structure via a stinger and a force gauge, and is driven by a white noise signal, filtered by a bandpass filter between 100 Hz and 3 kHz. Measurements of velocity are taken at the grid of points marked on the ABH taper using a laser doppler vibrometer.

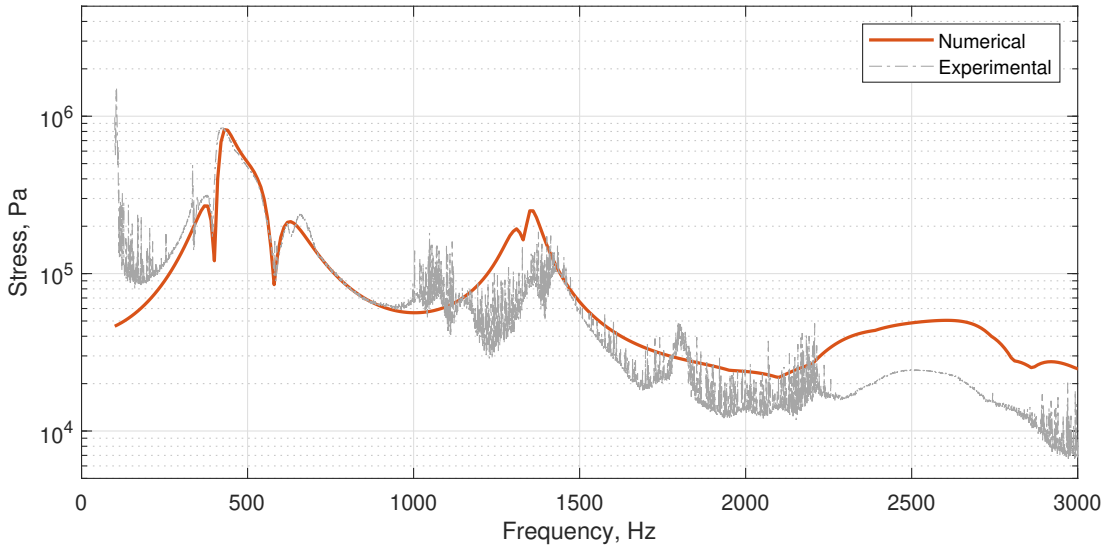

Figure 6: Stress against frequency plotted for the numerical results, direct (dashed line) and calculated (solid line), and for the calculated experimental results (dot-dashed line).

B. RESULTS

Measurements of the velocity across the ABH taper have been taken using the experimental set-up described in Section 4A, and the bending stress has then been calculated using the method outlined in Section 2. Due to the sensitive nature of the calculation of the second spatial derivative of beam deflection, a linear regression smoothing function has also been applied to the experimental data along the length of the ABH taper.

Figure 6 shows the experimentally calculated stress alongside the calculated stress from the numerical model. Examination of the results shows very good agreement between the numerical and experimental stress calculated around the first peak in the stress response at $300 - 700$ Hz. Outside of this frequency range the experimental data becomes more noisy, however, the shape of the second peak around 1300 Hz closely resembles that of the numerical calculation, although there is a noticeable shift in amplitude and frequency. It is thought that the reason for the differences between the experimental and numerical stress calculated results is mostly due to noise in the experimental data, since even a small amount of noise in the beam deflection data results in a large increase in the calculated stress due to the second derivative.

5. CONCLUSIONS

This paper has presented an investigation into a method proposed for the calculation of the stress in an ABH taper using velocity data from a grid of points across the structure. The accuracy of the proposed method has been assessed by comparing the calculated stress to the stress directly evaluated in the numerical model, and the results of the calculation have been validated experimentally.

The numerical assessment of ABH stress has shown that the calculation method proposed gives results where the shape of the stress response over frequency lines up well with the directly evaluated stress, but the calculation consistently underestimates the stress in the ABH taper. It is thought that this difference could be due to the assumptions made by Euler-Bernoulli beam theory, such as that of the beam having a constant thickness.

Experimental measurements of stress in an ABH taper are used to validate the numerical predictions

made, showing good agreement with numerical data, especially around the first peak in the stress response. The experimental data is quite noisy in places, however, this is due to the second spatial derivative of beam deflection amplifying the effect of noise in the measurements, despite attempting to minimise this effect by implementing a smoothing algorithm.

REFERENCES

[1] M. A. Mironov, "Propagation of a flexural wave in a plate whose thickness decreases smoothly to zero in a finite interval", *(in English) Soviet Physics Acoustics - USSR*, **34(3)**, 318–319 (1988).

[2] V. V. Krylov and F. J. B. S. Tilman, "Acoustic 'black holes' for flexural waves as effective vibration dampers", *Journal of Sound and Vibration*, **274(3)**, 605–619, (2004).

[3] K. Hook, J. Cheer and S. Daley, "A parametric study of an acoustic black hole on a beam", *J. Acoust. Soc. Am.*, **145(6)**, 3488–3498, (2019).

[4] P. Feurtado and S. Conlon, "Investigation of boundary-taper reflection for acoustic black hole design", *Noise Control Engineering Journal*, **63(5)**, 460–466, (2015).

[5] E. P. Bowyer and V. V. Krylov, "Slots of power-law profile as acoustic black holes for flexural waves in metallic and composite plates", *Structures*, **6**, 48–58, (2016).

[6] D. J. O'Boy and V. V. Krylov, "Vibration of a rectangular plate with a central power-law profiled groove by the rayleigh-ritz method", *Applied Acoustic*, **104**, 24–32, (2016).

[7] T. Zhou, L. L. Tang, H. L. Ji, J. H. Qiu and L. Cheng, "Dynamic and static properties of double-layered compound acoustic black hole structures", *Int. J. Applied Mechanics*, **9(5)**, (2017).

[8] A. Keys and J. Cheer, "Fatigue analysis of an acoustic black hole", *Proceedings of the 28th International Congress on Sound and Vibration*, (2022).

[9] A. Keys and J. Cheer, "Modified acoustic black hole profile for improved fatigue performance", *Proceedings of the 51st International Congress and Exposition on Noise Control Engineering*, (2022).

[10] V. V. Krylov and R. E. Winward, "Experimental investigation of the acoustic black hole effect for flexural waves in tapered plates", *Journal of Sound and Vibration*, **300**, (2007).

[11] W. C. Young and R. G. Budynas, "Roark's formulas for stress and strain", 7th ed., McGraw-Hill, (2002).